

**$\alpha$ -nucleus potential for  $\alpha$ -decay and sub-barrier fusion**V. Yu. Denisov<sup>1,2</sup> and H. Ikezoe<sup>1</sup><sup>1</sup>*Japan Atomic Energy Research Institute, Tokai, Ibaraki 319-1195, Japan*<sup>2</sup>*Institute for Nuclear Research, Prospect Nauki 47, 03680 Kiev, Ukraine*

(Received 5 July 2005; published 21 December 2005)

The set of parameters for  $\alpha$ -nucleus potential is derived by using the data for both the  $\alpha$ -decay half-lives and the fusion cross sections around the barrier for reactions  $\alpha + {}^{40}\text{Ca}$ ,  $\alpha + {}^{59}\text{Co}$ , and  $\alpha + {}^{208}\text{Pb}$ . The  $\alpha$ -decay half-lives are obtained in the framework of a cluster model using the WKB approximation. The evaluated  $\alpha$ -decay half-lives and the fusion cross sections agreed well with the data. Fusion reactions between  $\alpha$  particles and heavy nuclei can be used for both the formation of very heavy nuclei and spectroscopic studies of the formed compound nuclei.

DOI: [10.1103/PhysRevC.72.064613](https://doi.org/10.1103/PhysRevC.72.064613)

PACS number(s): 21.10.Tg, 21.60.Gx, 23.60.+e, 25.70.Jj

**I. INTRODUCTION**

Knowledge of the  $\alpha$ -nucleus interaction potential is key for the analysis of various reactions between  $\alpha$  particles and nuclei. By using the potential between  $\alpha$  particles and nuclei we can evaluate the cross sections for various reactions.

The  $\alpha$ -decay process involves sub-barrier penetration of  $\alpha$  particles through the barrier, caused by interactions between  $\alpha$  particles and nucleus. Therefore,  $\alpha$ -decay half-lives depend strongly on the  $\alpha$ -nucleus interaction potential as well.

The fusion reaction between  $\alpha$  particle and nucleus proceeds in the opposite direction of the  $\alpha$ -decay reaction. However, the same  $\alpha$ -nucleus interaction potential is the principal factor in describing both reactions. Therefore it is natural to use data for both the  $\alpha$ -decay half-lives and the sub-barrier fusion reactions for determination of the  $\alpha$ -nucleus interaction potential. Note that a combination of these data has not yet been used for evaluation of  $\alpha$ -nucleus potential.

The nucleus-nucleus interaction potential consists of both Coulomb repulsion and nuclear attraction parts. These two parts form a barrier at small distances between  $\alpha$  particles and nuclei. The Coulomb component of the potential is well known. In contrast, the nuclear part of the potential is less well defined. There are many different approaches to the nuclear part of the interaction potential between  $\alpha$  particles and nuclei [1–11].  $\alpha$ -decay [3,5–7,10] and various scattering [1,2,4,8,9] data are used for evaluation of the  $\alpha$ -nucleus potential. However, there are no global potentials between  $\alpha$  particles and nuclei that fit various reaction data from many nuclei at collision energies deeply below and around the barrier with good accuracy (e.g., the IAEA Reference Input Parameter Library [11]). Potentials [1–11] evaluated for the same colliding system using different approaches differ considerably. Thus, there is a need to reduce the uncertainty of the interaction potential around the point where the  $\alpha$  particle and nucleus touch at low collision energies.

The fusion reaction between the  $\alpha$  particles and nucleus at collision energies around the barrier is very sensitive to the behavior of the potential around the barrier. The energy released in the  $\alpha$ -decay transition from the ground state to the ground state is the  $Q$  value. The  $Q$  value of  $\alpha$  decay is smaller than the energies used in sub-barrier fusion reactions.

Therefore, the ground-state-to-ground-state  $\alpha$  decay of nuclei is sensitive to the values of potential over a very wide range of distances, from close to touching to very large. The distance between the  $\alpha$  particles and nucleus is reduced during the fusion process, whereas the distance increases in the case of  $\alpha$  decay of a nucleus. Thus, these reactions are the inverse of each other, and we should describe both reactions using the same potential. Therefore, data sets for both fusion and  $\alpha$  decay together present a unique opportunity for accurate determination of the  $\alpha$  nucleus potential at the energy range from close to zero to around the barrier. The knowledge of the  $\alpha$ -nucleus potential over this energy range is also very important for various other applications. For example, the evaluation of the  $\alpha$ -particle capture rate is very important for describing reactions in stars [6,8,12].

The low-energy fusion reactions and  $\alpha$  decays are related only to the real part of the potential. However, cross sections of various reactions at collision energies higher than the barrier depend on the both real and imaginary parts of the  $\alpha$ -nucleus potential [2,4,6,8,9]. Therefore, the fusion and  $\alpha$ -decay reactions present a unique opportunity to reduce the number of fitting parameters used in determining the real part of the  $\alpha$ -nucleus potential.

The experimental information on  $\alpha$ -decay half-lives is extensive and is being continually updated (see Refs. [3,7,13–18] and articles cited therein). The theory of  $\alpha$  decay was formulated by Gamow a long time ago [19]. Subsequently various microscopic [20–26], macroscopic cluster [3,5,7,10,18], and fission [13,27] approaches to the description of  $\alpha$  decay have been proposed. The simple empirical relations described the  $\alpha$ -decay half-lives [7,27–29] are discussed also. Below we use a cluster approach to the  $\alpha$  decay, which is the most suitable for determining the interaction potential between  $\alpha$  particles and the nucleus. Using this potential we simultaneously describe the available data for both the  $\alpha$ -decay half-lives and the sub-barrier fusion reaction cross sections.

Many  $\alpha$  emitters are deformed. Therefore  $\alpha$ -nucleus potential should depend on the angle  $\theta$  between the direction of  $\alpha$  emission and the axial-symmetry axis of the deformed nucleus. Both the  $\alpha$ -decay width and the transmission coefficient for tunneling through the barrier are strongly dependent on

$\theta$  [20,22–26,30–33]. This effect is considered in detail in microscopic models [23–26]. Unfortunately, deformation and angle effects have not been considered in previously discussed cluster models of  $\alpha$ -decay half-lives [3,5–7,10,13,18]. Below, we take into account the deformation of a daughter nucleus during  $\alpha$  decay within the framework of our simple cluster model.

The fusion reactions between nuclei around the barrier are strongly influenced by the coupling to both low-energy surface vibration states and nucleon transfers [34–37]. These two mechanisms of sub-barrier fusion enhancement are considered in detail in the construction of various models [34–37]. Unfortunately, the amplitude of this enhancement of sub-barrier fusion cross section varies depending on the model and various parameters. Moreover, some of these parameters are often used for data fitting. However, such coupling effects are small in the cases of stiff magic or near-magic nuclei. The neutron transfer enhancement of sub-barrier fusion cross section can be neglected when neutron transfer channels with positive  $Q$  value are absent [36]. We chose the fusion reactions  $\alpha + {}^{40}\text{Ca}$ ,  $\alpha + {}^{59}\text{Co}$ , and  $\alpha + {}^{208}\text{Pb}$  for evaluation of the  $\alpha$ -nucleus potential, because the magic or near-magic nuclei  ${}^4\text{He}$ ,  ${}^{40}\text{Ca}$ ,  ${}^{59}\text{Co}$ , and  ${}^{208}\text{Pb}$  are very stiff and all one- and two-nucleon transfer channels have negative  $Q$  values for these reactions. Thus, in these reactions the values of the sub-barrier fusion cross-sections evaluated by different models are very close to each other, and we can make a model-independent analysis of these reactions without fitting any additional parameters. Fortunately, there are experimental data for fusion reactions  $\alpha + {}^{40}\text{Ca}$ ,  $\alpha + {}^{59}\text{Co}$ , and  $\alpha + {}^{208}\text{Pb}$  [38–41].

Our cluster model for evaluation of  $\alpha$ -decay half-lives and sub-barrier fusion reaction is presented in Sec. II. The strategy for  $\alpha$ -nucleus potential parameters searching is described in Sec. III. The discussion of the results and our conclusions are given in Sec. IV.

## II. MODEL FOR $\alpha$ -DECAY AND SUB-BARRIER FUSION

The  $\alpha$ -decay half-life  $T_{1/2}$  is calculated as follows:

$$T_{1/2} = \hbar \ln(2) / \Gamma, \quad (1)$$

where  $\Gamma$  is the total width of decay. The  $\alpha$  particle can be emitted from any point of the nuclear surface and in any direction. It is obvious, however, that the  $\alpha$ -particle emission in a direction normal to the nuclear surface is the most profitable in terms of energy. Thus the total width is evaluated by averaging partial widths (see also Refs. [23,26]). Therefore the total  $\alpha$ -decay width is as follows:

$$\Gamma = \frac{1}{4\pi} \int \gamma(\theta, \phi) d\Omega, \quad (2)$$

where  $\gamma(\theta, \phi)$  is the partial width of  $\alpha$  emission in direction  $\theta$  and  $\phi$  and  $\Omega$  is the space angle. Note that similar averaging along the angle  $\Omega$  is also used for the evaluation of sub-barrier fusion cross sections between spherical and statically deformed nuclei [34,37] [see below Eq. (11)].

The majority of the ground-state  $\alpha$  emitters are spherical nuclei or axial-symmetric nuclei with moderate quadrupole

deformation. Therefore we simplify the expression for total width. It can be written as follows:

$$\Gamma = \int_0^{\pi/2} \gamma(\theta) \sin(\theta) d\theta, \quad (3)$$

where  $\theta$  is the angle between the symmetry axis of axially symmetric deformed nuclei and the vector from the center of the deformed nucleus to the emission point on the nuclear surface. Because of the small or moderate values of the quadrupole deformation of nuclei we neglect the difference between the surface normal direction and  $\theta$ . It is obvious that  $\Gamma = \gamma(\theta) = \gamma(0)$  for spherical nuclei.

The width of  $\alpha$  emission in direction  $\theta$  is given by the following:

$$\gamma(\theta) = \hbar \xi t(Q, \theta, \ell), \quad (4)$$

where  $\xi = \nu S$ ;  $\nu$  is the frequency of assaults of a  $\alpha$  particle on the barrier;  $S$  is the spectroscopic or preformation factor;  $t(Q, \theta, \ell)$  is the transmission coefficient, which shows the probability of penetration through the barrier; and  $Q$  is the released energy at  $\alpha$  decay.

The transmission coefficient can be obtained in the semi-classical WKB approximation

$$t(Q, \theta, \ell) = \left( 1 + \exp \left\{ \frac{2}{\hbar} \int_{a(\theta)}^{b(\theta)} dr \sqrt{2\mu[v(r, \theta, \ell, Q) - Q]} \right\} \right)^{-1}, \quad (5)$$

where  $a(\theta)$  and  $b(\theta)$  are the inner and outer turning points determined from the equations  $v(r, \theta, \ell, Q)|_{r=a(\theta), b(\theta)} = Q$  and  $\mu$  is the reduced mass. The  $\alpha$ -nucleus potential  $v(r, \theta, \ell, Q)$  consists of Coulomb  $v_C(r, \theta)$ , nuclear  $v_N(r, \theta, Q)$ , and centrifugal  $v_\ell(r)$  parts, i.e.,

$$v(r, \theta, \ell, Q) = v_C(r, \theta) + v_N(r, \theta, Q) + v_\ell(r). \quad (6)$$

We propose that the parts of  $\alpha$ -nucleus potential be written in the following form:

$$v_C(r, \theta) = \frac{2Ze^2}{r} \left[ 1 + \frac{3R^2}{5r^2} \beta Y_{20}(\theta) \right], \quad (7)$$

if  $r \geq r_m$ ,

$$v_C(r, \theta) \approx \frac{2Ze^2}{r_m} \left[ \frac{3}{2} - \frac{r^2}{2r_m^2} + \frac{3R^2}{5r_m^2} \beta Y_{20}(\theta) \left( 2 - \frac{r^3}{r_m^3} \right) \right], \quad (8)$$

if  $r \lesssim r_m$ ,

$$v_N(r, \theta, Q) = V(A, Z, Q) / (1 + \exp\{[r - r_m(\theta)]/d\}), \quad (9)$$

$$v_\ell(r) = \hbar^2 \ell(\ell + 1) / (2\mu r^2). \quad (10)$$

Here  $A$ ,  $Z$ ,  $R$ , and  $\beta$  are, respectively, the number of nucleons, the number of protons, the radius, and the quadrupole deformation parameter of the nucleus interacting with the  $\alpha$  particle;  $e$  is the charge of proton;  $Y_{20}(\theta)$  is the spherical harmonic function; and  $V(A, Z, Q, \theta)$  and  $r_m(\theta)$  are, respectively, the strength and effective radius of the nuclear part of  $\alpha$ -nucleus potential. The inner turning point  $a(\theta)$  is close to the touching point  $r_m(\theta)$ , and therefore the presentation of the Coulomb field

in the form shown in Eq. (8) at distances  $r \lesssim r_m(\theta)$  ensures the continuity of the Coulomb field and its derivative at  $r = r_m$ .

The trajectory of an  $\alpha$  particle emitted from a deformed nucleus is depicted by values of two coordinates  $r$  and  $\theta$ . An  $\alpha$  particle emitted during the ground-state-to-ground-state transition has, as a rule, zero value of the orbital momentum  $\ell = 0$  and negligible tangential velocity. Thus, we disregard the small effects of variation of the angle  $\theta$  during the barrier penetration in the case of  $\alpha$  emission from deformed nuclei. Therefore the action [Eq. (5)] related to the sub-barrier penetrability depends only on  $r$ .

The sub-barrier fusion cross section between spherical projectile and target nuclei with axial quadrupole deformation at collision energy  $E$  is equal to the following:

$$\sigma(E) = \frac{\pi \hbar^2}{2\mu E} \int_0^{\pi/2} \sum_{\ell} (2\ell + 1) t(E, \theta, \ell) \sin(\theta) d\theta \quad (11)$$

(see Refs. [34–37]). Here the integration on angle  $\theta$  is done for the same reason as for Eqs. (2) and (3). The transmission coefficient  $t(E, \theta, \ell)$  can be obtained using various sub-barrier fusion models [34–37]. We evaluated  $t(E, \theta = 0, \ell)$  using the semiclassical WKB approximation [Eq. (5)] in the case of collision between  $\alpha$  particle and stiff magic or near-magic spherical nuclei at collision energies  $E$  below barrier. The transmission coefficient is approximated by an expression for a parabolic barrier [34,36] at collision energies higher then or equal to the barrier energy.

### III. STRATEGY OF PARAMETERS SEARCHING

We chose data for  $T_{1/2}$  for 367  $\alpha$ -decay transitions between the ground states of parent and daughter nuclei from tables in Refs. [13,14,18]. There are 166 even-even, 84 even-odd, 67 odd-even, and 50 odd-odd parent nuclei among these 367  $\alpha$ -decay transitions.

The ground-state-to-ground-state  $\alpha$  transitions of even-even nuclei took place at  $\ell = 0$ . The value of  $\ell$  can be different from zero for the ground-state-to-ground-state transitions in odd or odd-odd nuclei. However, we assume that all  $\alpha$  transitions between the ground states of parent and daughter nuclei from Refs. [13,14,18] took place at  $\ell = 0$ , because information on value of  $\ell$  is absent in these data compilations. Similar approximation is also used in Refs. [5–7,13,18].

The  $\alpha$ -decay reaction  $Q$  values were evaluated using recent atomic mass data [42] or from Ref. [18] in the case of superheavy nuclei. The experimental data on static quadrupole deformation parameter  $\beta$  is taken from the RIPL-2 database [11]. However, if information on  $\beta$  for a nucleus is not given in this database, we picked up the value of  $\beta$  from Ref. [43].

The data for sub-barrier fusion cross sections for reactions  $\alpha + {}^{40}\text{Ca}$ ,  $\alpha + {}^{59}\text{Co}$ , and  $\alpha + {}^{208}\text{Pb}$  were taken from Refs. [38–41]. We wanted to describe both the half-lives for 367  $\alpha$  decays and fusion cross sections for reactions  $\alpha + {}^{40}\text{Ca}$ ,  $\alpha + {}^{59}\text{Co}$ , and  $\alpha + {}^{208}\text{Pb}$  by using Eqs. (1)–(11). By solving this task we determined the parameters  $V(A, Z, Q)$ ,  $r_m(\theta)$ , and  $d$  of the nuclear part of the  $\alpha$ -nucleus potential [Eq. (9)].

In determining the parameter values of the potential we took into account the fact that various data are known with different

accuracy. The most accurate data are those of the ground-state-to-ground-state  $\alpha$  transitions in even-even nuclei. The data for similar transitions in odd-even or even-odd or odd-odd nuclei are less accurate as a rule, because of uncertainty of  $\ell$ , the level schemes of parent and/or daughter nuclei and other reasons. The data for fusion reactions is less accurate than data for  $\alpha$ -decay half-lives as a rule. Furthermore, there are two sets of data [38,39] for the fusion reaction  $\alpha + {}^{40}\text{Ca}$  that do not agree well with each other.

Therefore we estimated the parameter values of the potential starting from both data of the  $\alpha$ -decay half-lives  $T_{1/2}$  of spherical and slightly deformed ( $|\beta| \leq 0.05$ ) nuclei and data of the fusion reaction cross sections. Next we identified specific features relating to the description of  $T_{1/2}$  in deformed nuclei.

At the very beginning of our study we tried to describe data for  $\log_{10}(T_{1/2})$  in even-even nuclei without taking into account the fusion data. We tried to minimize the difference

$$D_{e-e} = \sum_{e-e \text{ nuclei}} [\log_{10}(T_{1/2}^{\text{theor}}) - \log_{10}(T_{1/2}^{\text{expt}})]^2, \quad (12)$$

where  $T_{1/2}^{\text{theor}}$  and  $T_{1/2}^{\text{expt}}$  are theoretical and experimental values of half-lives respectively. However, we could not fix the parameters of  $\alpha$ -nucleus potential, because it is possible to describe  $\log_{10}(T_{1/2})$  in even-even nuclei with similar values of root-mean-square error using very different values of nuclear potential strength  $V(A, Z, q, \theta)$ , diffuseness  $d$ , radii  $r_m$ , and  $\xi$ . Note that this situation is typical. The values of  $\log_{10}(T_{1/2})$  are well described in Refs. [3,5–7,13,27]; however, the values of potential strength, diffuseness, radii, and  $\xi$  in these references vary by large intervals.

Subsequently, we tried to describe simultaneously data for  $\log_{10}(T_{1/2})$  in even-even, even-odd, odd-even, and odd-odd nuclei as well as for the sub-barrier fusion data for the reaction  $\alpha + {}^{208}\text{Pb}$ . We paid special attention to the description of  $\log_{10}(T_{1/2})$  in even-even data, and therefore for our parameter searching we tried to minimize the function

$$100D_{e-e} + D_{e-o} + D_{o-e} + D_{o-o} + \sum_k [\sigma_{\text{fus}}^{\text{theor.}}(E_k) - \sigma_{\text{fus}}^{\text{expt.}}(E_k)]^2. \quad (13)$$

Here  $D_{e-o}$ ,  $D_{o-e}$ , and  $D_{o-o}$  are the differences similar to Eq. (12) for even-odd, odd-even, and odd-odd data sets correspondingly, and  $\sigma_{\text{fus}}^{\text{theor.}}(E_k)$  and  $\sigma_{\text{fus}}^{\text{expt.}}(E_k)$  are theoretical and experimental values of fusion cross section at energy  $E_k$  for reaction  $\alpha + {}^{208}\text{Pb}$  respectively. We took into account all data on cross sections of the reaction  $\alpha + {}^{208}\text{Pb}$ . The values of fusion cross section during the minimization procedure are expressed in millibarns. The experimental errors in sub-barrier fusion cross-section values are raised with reduction of collision energy, especially in the sub-barrier region [38–41]. This is taken into account in Eq. (13).

The quality of description of  $\alpha$ -decay half-lives is weakly influenced by the last term in Eq. (13). However, by using this approach we remove the freedom in the choice of parameter  $\xi$ . The value of parameter  $\xi$  is coupled to the parameters of the potential in this step. Nevertheless, we cannot strictly determine the parameters of the potential, because we may describe target data sets with comparable values of

root-mean-square-error using very different values of nuclear potential strength  $V(A, Z, q, \theta)$ .

The additional demand that the parameters describe the cross section data for fusion reactions  $\alpha + {}^{40}\text{Ca}$  and  $\alpha + {}^{59}\text{Co}$  as well as the previous target data sets make it possible to fix the parameters of the nuclear part of the potential between  $\alpha$ -particle and spherical nuclei. Note that the data sets for fusion cross sections for reactions  $\alpha + {}^{40}\text{Ca}$  and  $\alpha + {}^{59}\text{Co}$  are known to have lower accuracy than other data sets, and therefore for parameter searching we give very small factors to the terms related to the difference between theoretical and experimental cross sections, which we add to the function [Eq. (13)]. These small factors reasonably diminish the influence of fusion data sets for the reactions  $\alpha + {}^{40}\text{Ca}$  and  $\alpha + {}^{59}\text{Co}$ .

The obtained values of parameters are as follows.

$$V(A, Z, Q) = -[30.275 - 0.45838Z/A^{1/3} + 58.270I - 0.24244Q], \quad (14)$$

$$r_m = 1.5268 + R, \quad (15)$$

$$R = R_p(1 + 3.0909/R_p^2) + 0.12430t, \quad (16)$$

$$R_p = 1.24A^{1/3}(1 + 1.646/A - 0.191I), \quad (17)$$

$$t = I - 0.4A/(A + 200), \quad (18)$$

$$d = 0.49290, \quad (19)$$

$$\xi = (6.1814 + 0.2988A^{-1/6})10^{19} \text{ s}^{-1}, \quad (20)$$

where  $I = (A - 2Z)/A$ . Here we use a method for determining the radius parameters similar to that used in Ref. [44] for evaluating the nuclear part of the potential between two heavy spherical nuclei. The quality of description of fusion reactions  $\alpha + {}^{40}\text{Ca}$  and  $\alpha + {}^{59}\text{Co}$  is degraded for other sets of potential parameters.

The density distribution of a deformed nucleus is described by deformation parameter  $\beta$  and angle  $\theta$ . Therefore, the potential between the  $\alpha$  particle and deformed nucleus should depend on deformation  $\beta$  and angle  $\theta$ , because the nuclear part of the potential is strongly linked to nucleon density in the double-folding model [44,45]. It is natural that the parameter values determining the  $\alpha$ -nucleus potential do not change with the transition from a spherical to a deformed nucleus. Therefore, the angular dependence of the potential between an  $\alpha$  particle and a deformed nucleus can be linked to the density distribution of a deformed nucleus. As a result, the relation between deformation of the nucleus and angular dependence of the nuclear part of  $\alpha$ -nucleus potential can be associated with the radius parameters, i.e.,

$$r_m(\theta) = 1.5268 + R(\theta), \quad (21)$$

$$R(\theta) = R[1 + \beta Y_{20}(\theta)]. \quad (22)$$

The height of the barrier between the  $\alpha$  particle and the deformed nucleus and the inner turning point  $a(\theta)$  become strongly dependent on  $\theta$ . The dependence of potential on angle  $\theta$  is similar to that in the case of heavier nuclei [45]. The barrier between an  $\alpha$  particle and a prolate nucleus is lower and thinner at  $\theta = 0^\circ$  than at  $\theta = 90^\circ$ . Because of this the transmission coefficient  $t(q, \theta = 0^\circ, \ell)$  in a prolate nucleus is larger than the transmission coefficient in a spherical nucleus

where other parameters have the same values. As a result the evaluated half-lives of prolate nuclei are strongly reduced when we take into account the deformation of nuclei (see also Fig. 1 in Ref. [24]). However, the  $\alpha$ -decay hindrance caused by deformation of nuclei [26] strongly affects  $\alpha$ -decay half-lives.

For the sake of fitting data for half-lives of deformed nuclei we introduce a deformation dependence parameter  $\xi$

$$\xi = (6.1814 + 0.2988A^{-1/6})10^{19} \exp(-13.116\beta) \text{ s}^{-1}. \quad (23)$$

Note that  $\xi$  is the product of the assault frequency and the formation probability of the  $\alpha$ -particle cluster in the parent nucleus. The exponential factor in Eq. (23) reflects the fact that deformation strongly influences the formation probability of the  $\alpha$  cluster in the parent nucleus. Note that the deformation or angular dependency of the  $\alpha$ -nucleus potential near the inner turning point  $a(\theta)$  may slightly affect the assault frequency because of the variation of the  $\alpha$ -nucleus potential. This exponential factor reflects the hindrance of the  $\alpha$ -cluster formation in prolate nuclei and the enhancement of that in oblate nuclei. It is significant to note that the deformation-dependent exponential factor is also adopted in detailed microscopical  $\alpha$ -decay theories [23–26].

It is obvious that violation of spherical symmetry leads to modification of  $\alpha$ -particle localization on the surface of the deformed nucleus. Because of static quadrupole deformation the strong coupled-channel effect between outgoing waves with  $\ell = 0, 2, 4$  can also attenuate  $\ell = 0$   $\alpha$ -particle transitions in prolate nuclei [23–25]. Note that the transmission coefficient and half-life are strongly reduced with rising of  $\ell$  because of the centrifugal term described in Eqs. (6) and (10). For these reasons the introduction of the exponential factor in Eq. (23) is natural. However, it is desirable to discuss this exponential factor in detail in the light of microscopical considerations.

Note that  $t(q, \theta = 0^\circ, \ell) > t(q, \theta = 90^\circ, \ell)$  in prolate nuclei. Therefore, if we propose the independence of  $\alpha$ -cluster formation probability on the angle  $\theta$ , then the  $\alpha$  particles should be emitted mainly at angle  $\theta = 0^\circ$  (see also Refs. [23,25,30–33]). A similar effect is well known in the case of sub-barrier fusion reactions between spherical and deformed nuclei [34,37].

#### IV. RESULTS AND DISCUSSIONS

The results of our evaluations of various data are presented in Figs. 1–3. We start our discussion with detailed consideration of the  $\alpha$ -decay half-lives in nuclei.

##### A. $\alpha$ -decay half-lives

The  $\alpha$ -decay half-lives evaluated by using Eqs. (1)–(10) and (14)–(23) agree well with experimental data (see Figs. 1–2). The values of half-lives are scattered over an extremely wide range from  $\approx 10^{-7}\text{s}$  to  $\approx 10^{+25}\text{s}$ . The  $\alpha$ -decay half-lives are very nicely described in the case of even-even parent nuclei. We see in Fig. 1 that the difference between theoretical and experimental values of  $\log_{10} T_{1/2}$  are smaller than 0.5 for most of cases of even-even, even-odd, and odd-even nuclei. For odd-odd nuclei it is a little bit worse.

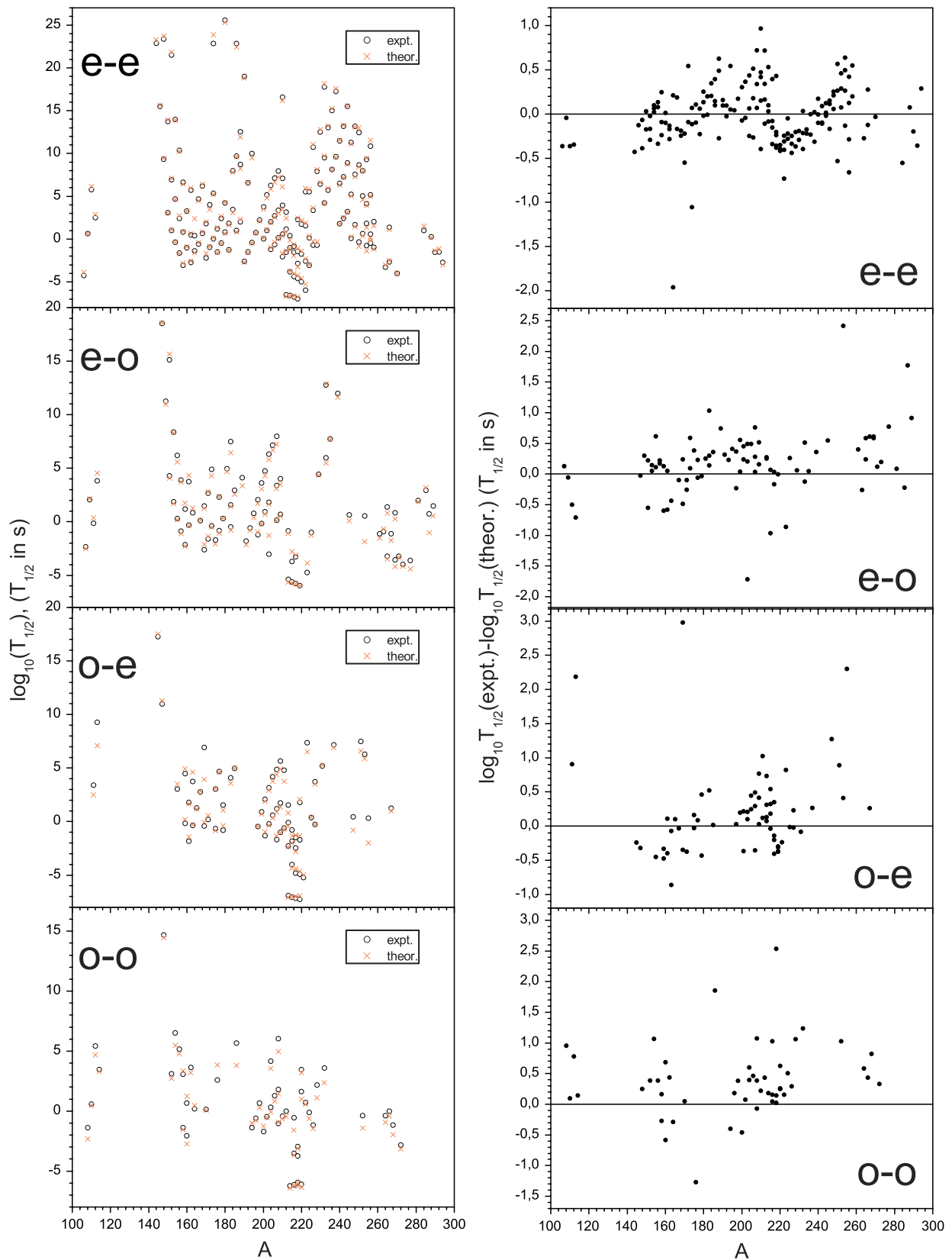


FIG. 1. (Color online) (Left panels) The experimental (circles) [13,14,18] and theoretical (crosses) values of  $\log_{10}(T_{1/2})$  for  $\alpha$  decays in even-even (e-e), even-odd (e-o), odd-even (o-e), and odd-odd (o-o) parent nuclei. (Right panels) Dots represent the difference between the experimental and theoretical values of  $\log_{10}(T_{1/2})$  for  $\alpha$  decays in even-even (e-e), even-odd (e-o), odd-even (o-e), and odd-odd (o-o) parent nuclei.

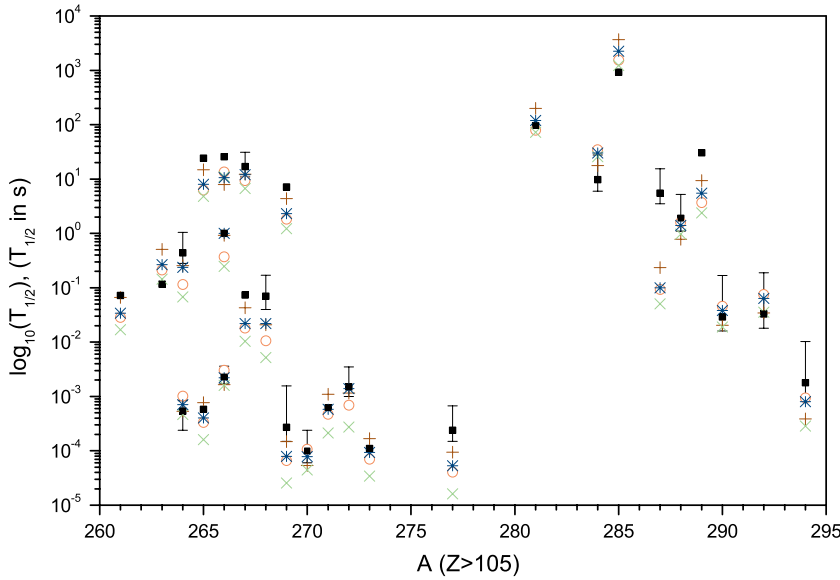


FIG. 2. (Color online) The experimental and theoretical values of  $\log_{10}(T_{1/2})$  for superheavy region. Squares with error bars are data from Refs. [13,18], circles are theoretical values obtained by using Eqs. (1)–(9) and (11)–(17), plus and cross signs are the values obtained by using empirical relations from Refs. [7] and [28] respectively, and stars are the results of calculations from Ref. [18].

The  $\alpha$  particles emitted from superheavy elements are considered in recent references [7,16,18,28]. In Fig. 2 we present the results for  $\log_{10}(T_{1/2})$  of superheavies using our model and other approaches [7,18,28]. Our results and those from Ref. [18] are obtained by use of different cluster model approaches to the  $\alpha$ -decay, whereas results from Refs. [7,28] are evaluated with the help of various empirical relations. The empirical relations used in Refs. [7,27–29] couple  $\log_{10}(T_{1/2})$ ,  $\alpha$ -particle  $Q$  value, mass, and charge of parent nuclei by simple functional expressions. As a rule, empirical relations are derived by using a pure Coulomb picture of  $\alpha$  decay, which neglects both the nuclear force between  $\alpha$  particle and daughter nucleus and the deformation of daughter nucleus [29]. Nevertheless the empirical relations are often used to

estimate  $\log_{10}(T_{1/2})$  because of their simplicity. The empirical relation from Ref. [28] was derived especially for describing  $\log_{10}(T_{1/2})$  in heavy and superheavy nuclei. In Ref. [7] four empirical relations for even-even, even-odd, odd-even, and odd-odd  $\alpha$ -decaying nuclei are established.

We see in Fig. 2 that our approximation describes  $\log_{10}(T_{1/2})$  for the superheavy region better than the empirical relation from Ref. [28] and worse than the set of empirical relations from Ref. [7]. The cluster theory proposed in Ref. [18] describes well  $\log_{10}(T_{1/2})$  in this region too. However, a renormalization factor for the nuclear part of  $\alpha$ -nucleus potential is used for each decay case in Ref. [18]. In contrast to this, our model describes well the half-lives of nuclei in a very wide region with the same set of potential parameters (see Figs. 1 and 2) and takes into account the deformation effects that are omitted in other approaches.

## B. Fusion cross sections

The fusion cross sections evaluated using Eqs. (5)–(11) and (14)–(19) for reactions  $\alpha + {}^{40}\text{Ca}$ ,  $\alpha + {}^{59}\text{Co}$ , and  $\alpha + {}^{208}\text{Pb}$  are compared with experimental data [38–41] shown in Fig. 3. We see that our model very accurately describes the data for the fusion reaction  $\alpha + {}^{208}\text{Pb}$ . The data for the reactions  $\alpha + {}^{40}\text{Ca}$  and  $\alpha + {}^{59}\text{Co}$  are also well described by our model.

Our model for evaluating the fusion cross section between an  $\alpha$  particle and a spherical nucleus is one dimensional. As pointed out in the Introduction, the coupled-channel effects are very important for the nuclear fusion reaction around the barrier [34–37]. Thus, we determined the coupled-channel calculation of the fusion cross-section for the reaction  $\alpha + {}^{208}\text{Pb}$  using CCFULL code [35], and the results are presented in Fig. 3. The effects of nonlinear coupling of the low-energy surface vibrational states in all orders are taken into account in this code. The CCFULL calculation uses the same  $\alpha$ -nucleus potential as in the case of one-dimensional calculation. The values of excitation energies and dynamic surface deformations are taken from Ref. [11]. As shown in Fig. 3, the

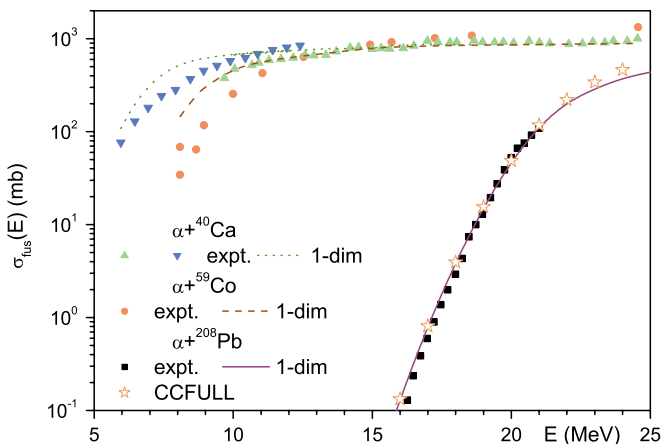


FIG. 3. (Color online) The experimental and theoretical values of fusion cross sections for reactions  $\alpha + {}^{40}\text{Ca}$ ,  $\alpha + {}^{59}\text{Co}$ , and  $\alpha + {}^{208}\text{Pb}$ . Squares are the data for the reaction  $\alpha + {}^{208}\text{Pb}$  from Ref. [41], circles are the data for the reaction  $\alpha + {}^{59}\text{Co}$  from Ref. [40], up- and down-pointing triangles are the data for the reaction  $\alpha + {}^{40}\text{Ca}$  from Refs. [39] and [38], respectively. Lines are results of calculations obtained by using Eqs. (5)–(11) and (14)–(19), and stars are the result of calculations using CCFULL code [35].

agreement between our one-dimensional and coupled-channel calculations is rather good. The good agreement between the CCFULL and one-dimensional calculations can be attributed to both the high stiffness of double-magic nuclei participating in this reaction and the smaller values of the  $\alpha$ -nucleus potential and its derivative than in the case of a more symmetric colliding system.

### C. Comparison with other approaches

The value of the depth  $V(A, Z, Q)$  [Eq. (14)] of the nuclear part of the  $\alpha$ -nucleus potential evaluated in our model is smaller than that typically obtained using data for high-energy reactions or some calculation from M3Y nucleon-nucleon forces [2,6,9]. However, the depth of the potential is unimportant in analyzing reaction data around the barrier. For example, it is possible to obtain  $\alpha$ -particle elastic scattering and total reaction cross-section data from either the deep or shallow nuclear part of the  $\alpha$ -nucleus potential using the optical model [1].

Small values of the depth of the nuclear part of the  $\alpha$ -nucleus potential are derived in the analysis of the low-energy data as a rule. Thus, good estimation of the  $\alpha$ -decay half-lives for superheavy nuclei in Ref. [18] (see also Fig. 2) is obtained by strong reduction of the nuclear part of the potential calculated from the M3Y nucleon-nucleon force. The strength of the nuclear part of  $\alpha$ -nucleus potential obtained in Ref. [7] is even smaller than that obtained by use of our approach (see Fig. 4).

The  $\alpha$ -decay and sub-barrier fusion processes are slow. The strong repulsion arises between nuclei at low collision energies because of the Pauli principle [46,47]. As a result, the  $\alpha$ -nucleus potential evaluated using the M3Y nucleon-nucleon force becomes shallower because of the Pauli repulsion. The depth of Woods-Saxon type potential is approximately less by half than the depth of M3Y type potential evaluated for the same  $\alpha$ -nucleus system, when both potentials are close

to each other at large distances [47]. Therefore the shallow  $\alpha$ -nucleus potential is reasonable for study of both  $\alpha$ -decay and sub-barrier fusion.

Our value of potential diffuseness [Eq. (19)] is smaller than those from Refs. [1,2,5,7,9]. The diffuseness of potential in the double-folding model is related to both the diffuseness of density distribution of interacting nuclei and the diffuseness of nucleon-nucleon force. The diffuseness of  $\alpha$  particles is small because the density distribution of the  $\alpha$  particles is close to Gaussian (see examples in Refs. [8,9]). As a rule, the diffuseness of density distribution in heavy nuclei does not depend on mass number. Therefore, the mass-independent small value of diffuseness obtained in our study is reasonable.

The expression for effective nuclear radius  $R$  is close to the one used in Ref. [44] for evaluation of the potential between two nuclei. The expression for proton radius  $R_p$  (14) is proposed in Ref. [48]. The value of the  $\alpha$ -particle radius, 1.5268 fm [see Eq. (15)], is very close to the experimental value  $1.57 \pm 0.05$  fm [49]. Note that during potential parameter searching, the value of the  $\alpha$ -particle radius is scanned in the interval from 0.5 to 2.0 fm.

The comparison of the nuclear part of the potentials at distance larger than touching point evaluated using our and other [2,5,7,9] approaches is presented in Fig. 4. The potentials for  $\alpha + {}^{40}\text{Ca}$  and  $\alpha + {}^{208}\text{Pb}$  are evaluated at  $E = 20$  MeV. We see in this figure that our potential is very close to the potentials from Refs. [2,5,9] near the touching points for  $\alpha + {}^{208}\text{Pb}$ . At larger distances between nuclei our potential is less attractive than that of the others. However, our potential is more attractive than those of the others [2,5,7,9] for the  $\alpha + {}^{40}\text{Ca}$  reaction; see Fig. 4. Here we should note that potential parametrizations from Refs. [2,5,9] are obtained by using data of interactions between  $\alpha$  and medium or heavy nuclei. The potential evaluated in Ref. [7] is less attractive than that of the others at distances close to the touching point.

### D. Fusion for superheavy element spectroscopy studies

Recently the fusion reactions between heavy nuclei have been used for spectroscopy studies of superheavy elements [16,50]. The cross sections of reactions used for this purpose are very small [50], because of compound-nucleus formation hindrance [17]. However, the fusion hindrance between  $\alpha$  particles and very heavy nuclei is absent, because of the small value of  $2Z$ , where 2 is the charge of the  $\alpha$  particle and  $Z$  is the charge of heavy nucleus. Therefore fusion reactions between  $\alpha$ -particle projectiles and very heavy target nuclei can be also used for heavy nucleus spectroscopy studies. It is possible to make spectroscopy studies of a compound nucleus on modern facilities if the compound-nucleus cross section is larger than  $0.2 \mu\text{b}$  [50].

We present the fusion cross section for the reaction  $\alpha + {}^{252}\text{Cf} = {}^{256}\text{Fm}$  evaluated by using Eqs. (5)–(11) and (14)–(19) in Fig. 5. The compound-nucleus cross section shown in Fig. 5 is evaluated for different proposed shapes of  ${}^{252}\text{Cf}$ . The spherical  ${}^{252}\text{Cf}$  cross section is smaller than the deformed one. Similar results are also found for the fusion

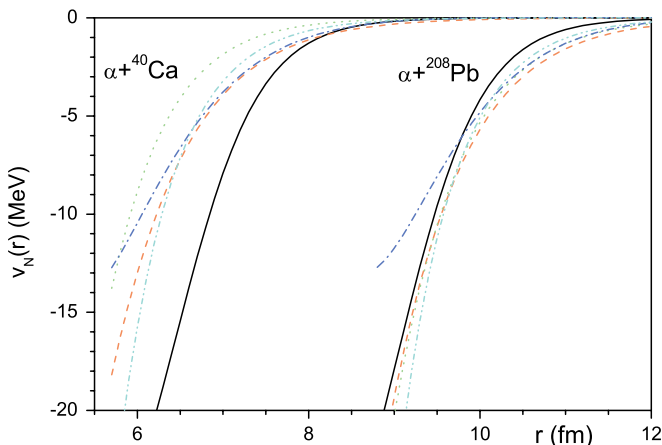


FIG. 4. (Color online) The nuclear part of potentials between  $\alpha$  particles and  ${}^{40}\text{Ca}$  or  ${}^{208}\text{Pb}$ . The solid, dash, dots, dash-dot, and dash-dot-dot lines are evaluation results using our model and parametrizations from Refs. [2,5,7,9], respectively.

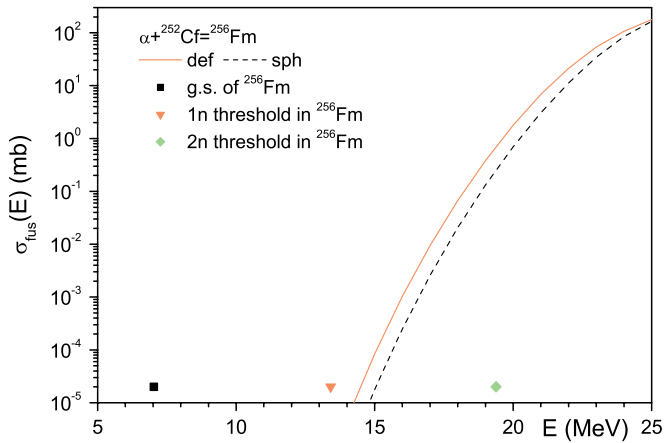


FIG. 5. (Color online) The fusion cross section for  $\alpha + {}^{252}\text{Cf} = {}^{256}\text{Fm}$  reactions. The solid and dashed lines are fusion cross sections in the cases of deformed and spherical shape of  ${}^{252}\text{Cf}$  respectively. The square marks the collision energy at which  ${}^{256}\text{Fm}$  is formed in the ground state. The triangle and diamond are threshold energies for one- and two- neutron emissions from  ${}^{256}\text{Fm}$ , respectively.

reactions between heavier projectiles and lighter targets [34,37]. The value of quadrupole deformation parameter for  ${}^{252}\text{Cf}$  is taken from Ref. [11]. From Fig. 5 we see that it is possible to make spectroscopy studies of  ${}^{256}\text{Fm}$  at collision energies  $E \gtrsim 16$  MeV. The excitation energies of  ${}^{256}\text{Fm}$  compound nuclei at such collision energies are moderate.

Note that we evaluate the fusion cross section by using the one-dimensional WKB approximation for the reaction between spherical and deformed nuclei. Coupling to the low-energy vibrational states in  ${}^{252}\text{Cf}$  can slightly increase the cross section values presented in Fig. 5. Because of this, our estimation of the cross section is the lower limit.

The spectroscopy studies of  ${}^{255}\text{Fm}$  can be made after  $1n$  emission from  ${}^{256}\text{Fm}$ . The neutron separation energy in  ${}^{256}\text{Fm}$  is  $E_{1n} = 6.4$  MeV [42] and the experimental fission barrier is  $E_f = 4.8$  MeV [51]. The compound-nucleus survival probability  $W$  is related to neutron emission  $\Gamma_n(E^*)$  and fission  $\Gamma_f(E^*)$  widths, i.e.,  $W \approx \Gamma_n(E^*)/\Gamma_f(E^*)$  [52]. These widths

are proportional to the level densities ratio, and therefore

$$W(E^*) \propto \exp\{2[a(E^* - E_n)]^{1/2} - 2[a(E^* - E_f)]^{1/2}\}, \quad (24)$$

where  $E^*$  is the excitation energy of the compound nucleus and  $a = 0.114A + 0.162A^{2/3}$  is the asymptotic level density parameter in a nucleus with  $A$  nucleons [53]. We see in this figure that the cross section for  ${}^{256}\text{Fm}$  formation at an energy level just below the  $2n$  emission threshold ( $E \approx 19$  MeV) is close to 0.4 mb. The compound-nucleus survival probability  $W$  at this excitation energy is  $W \approx 0.02$ . Therefore the cross section of the  $\alpha + {}^{252}\text{Cf} = {}^{255}\text{Fm} + 1n$  reaction is  $\sigma_{\text{fus}}(E)W(E - Q) \approx 8\mu\text{b}$ . Here we take into account that the excitation energy of compound-nucleus  ${}^{256}\text{Fm}$  formed in the fusion reaction  $\alpha + {}^{252}\text{Cf}$  at collision energy  $E$  is  $E^* = E - Q$ . The value of the cross section is high enough for spectroscopic studies of  ${}^{255}\text{Fm}$ .

The fusion reactions induced by  $\alpha$  particles have  $1n$  channels as a rule. In contrast to this, more neutrons are generally evaporated in the reactions between heavier projectiles and lighter targets leading to the same compound-nucleus formed in reactions induced by an  $\alpha$  projectile. However, the poor availability of heavy targets limits the use of  $\alpha$ -capture reactions. Nevertheless, the cross sections of these reactions are relatively high, and therefore these reactions are attractive for spectroscopic studies.

In conclusion, we determined the  $\alpha$ -nucleus potential by using the data for  $\alpha$ -decay half-lives and sub-barrier fusion reactions. The data for  $\alpha$ -decay half-lives play a principal role in potential evaluation. The data for  $\alpha$ -decay half-lives in spherical and deformed nuclei and for sub-barrier fusion reactions  $\alpha + {}^{40}\text{Ca}$ ,  $\alpha + {}^{59}\text{Co}$ , and  $\alpha + {}^{208}\text{Pb}$  are well described by our model. We showed that it is possible to use  $\alpha$ -nucleus fusion reactions for the spectroscopic studies of very heavy nuclei. The sub-barrier  $\alpha$ -capture reactions can be fruitfully used for the spectroscopy studies of very heavy nuclei.

#### ACKNOWLEDGMENTS

V. Yu. Denisov thanks the Japan Society for the Promotion of Science for its financial support.

- [1] J. R. Huizenga and G. Igo, Nucl. Phys. **29**, 462 (1962).
- [2] M. Nolte, H. Machner, and J. Bojowald, Phys. Rev. C **36**, 1312 (1987).
- [3] B. Buck, A. C. Merchant, and S. M. Perez, Phys. Rev. C **45**, 2247 (1992); At. Data Nucl. Data Tables **54**, 53 (1993).
- [4] U. Atzrott, P. Mohr, H. Abele, C. Hillenmayer, and G. Staudt, Phys. Rev. C **53**, 1336 (1996).
- [5] R. Blendowske, T. Fliessbach, and H. Walliser, in *Nuclear Decay Modes* (Institute of Physics, Bristol, 1996), p. 337.
- [6] P. Mohr, Phys. Rev. C **61**, 045802 (2000).
- [7] R. Moustabchir and G. Royer, Nucl. Phys. **A683**, 266 (2001).
- [8] P. Demetriou, C. Grama, and S. Goriely, Nucl. Phys. **A707**, 253 (2002).
- [9] M. Avrigeanu, W. von Oertzen, A. J. M. Plompen, and V. Avrigeanu, Nucl. Phys. **A723**, 104 (2003).
- [10] D. N. Basu, Phys. Lett. **B566**, 90 (2003).
- [11] <http://www-nds.iaea.org/RIPL-2/>
- [12] T. Rauscher, F.-K. Thielemann, J. Görres, and M. Wiescher, Nucl. Phys. **A675**, 695 (2000).
- [13] S. B. Duarte, O. A. P. Tavares, F. Guzman, A. Dimarco, F. Garcia, O. Rodriguez, and M. Goncalves, At. Data Nucl. Data Tables **80**, 235 (2002).
- [14] F. A. Danevich, A. S. Georgadze, V. V. Kobychyev, S. S. Nagorny, A. S. Nikolaiko, O. A. Ponkratenko, V. I. Tretyak, S. Yu. Zdesenko, Yu. G. Zdesenko, P. G. Bizzeti, T. F. Fazzini, and P. R. Maurenzig, Phys. Rev. C **67**, 014310 (2003).
- [15] K. Nishio, H. Ikezoe, S. Mitsuoka, K. Satou, and C. J. Lin, Phys. Rev. C **68**, 064305 (2003).
- [16] S. Hofmann and G. Münzenberg, Rev. Mod. Phys. **72**, 733 (2000).
- [17] P. Armbruster, Annu. Rev. Nucl. Part. Sci. **50**, 411 (2000).

- [18] C. Xu and Z. Ren, Nucl. Phys. **A753**, 174 (2005).
- [19] G. Gamow, Z. Phys. **51**, 204 (1928).
- [20] R. G. Lovas, R. J. Liotta, A. Insolia, K. Varga, and D. S. Delion, Phys. Rep. **294**, 265 (1998).
- [21] S. G. Kadenskii and V. I. Furman, Sov. J. Part. Nucl. **6**, 189 (1976) (in English).
- [22] S. G. Kadenskii, V. E. Kalechits, and A. A. Martynov, Sov. J. Nucl. Phys. **14**, 193 (1972) (in English).
- [23] T. L. Stewart, M. W. Kermode, D. J. Beachey, N. Rowley, I. S. Grant, and A. T. Kruppa, Nucl. Phys. **A611**, 332 (1996).
- [24] D. S. Delion, A. Insolia, and R. J. Liotta, Phys. Rev. C **49**, 3024 (1994).
- [25] D. S. Delion, A. Insolia, and R. J. Liotta, Phys. Rev. C **46**, 1346 (1992); **67**, 054317 (2003).
- [26] A. Bohr and B. R. Mottelson, *Nuclear Structure* (Benjamin, New York, 1975), Vol. 2.
- [27] D. P. Poenaru, E. Hourani, and W. Greiner, in *Nuclear Decay Modes* (Institute of Physics, Bristol, 1996), p. 204.
- [28] R. Smolanczuk, J. Skalski, and A. Sobczewski, in *Proceedings of the International Workshop XXIV on Gross Properties of Nuclei and Nuclear excitations "Extremes of Nuclear Structure," Hirschegg, Austria, 1996*, edited by H. Feldmeier, J. Knoll, and W. Nörenberg (GSI, Darmstadt, 1996), p. 35.
- [29] B. A. Brown, Phys. Rev. C **46**, 811 (1992).
- [30] V. P. Aleshin, Part. Nucl. **21**, 963 (1990) (in Russian); Sov. J. Part. Nucl. **21**, 407 (1990) (in English); Nucl. Phys. **A605**, 120 (1996).
- [31] N. N. Ajitanand, G. La Rana, R. Lacey, D. J. Moses, L. C. Vaz, G. F. Peaslee, D. M. de Castro Rizzo, M. Kaplan, and J. M. Alexander, Phys. Rev. C **34**, 877 (1986).
- [32] J. R. Huizenga, A. N. Behkami, I. M. Govil, W. U. Schröder, and J. Toke, Phys. Rev. C **40**, 668 (1989).
- [33] N. Severijns, A. A. Belyaev, A. L. Erzikyan, P.-D. Eversheim, V. T. Filimonov, V. V. Golovko, G. M. Gurevich, P. Herzog, I. S. Kraev, A. A. Lukhanin, V. I. Noga, V. P. Parfenova, T. Phalet, A. V. Rusakov, Yu. G. Toporov, C. Tramm, V. N. Vyachin, D. Zakoucky, and E. Zotov, Phys. Rev. C **71**, 044324 (2005).
- [34] M. Dasgupta, D. J. Hinde, N. Rowley, and A. M. Stefanini, Annu. Rev. Nucl. Part. Sci. **48**, 401 (1998).
- [35] K. Hagino, N. Rowley, and A. T. Kruppa, Comput. Phys. Commun. **123**, 143 (1999).
- [36] V. Yu. Denisov, Phys. At. Nucl. **62**, 1349 (1999); Eur. Phys. J. **A7**, 87 (2000).
- [37] J. O. Fernandez-Niello, C. H. Dasso, and S. Landowne, Comput. Phys. Commun. **54**, 409 (1989).
- [38] K. A. Eberhard, Ch. Appel, R. Bangert, L. Cleemann, J. Eberth, and V. Zobel, Phys. Rev. Lett. **43**, 107 (1979).
- [39] J. John, C. P. Robinson, J. P. Aldridge, and R. H. Davis, Phys. Rev. **177**, 1755 (1969).
- [40] J. M. D'Auria, M. J. Fluss, L. Kowalski, and J. M. Miller, Phys. Rev. **168**, 1224 (1968).
- [41] A. R. Barnett and J. S. Lilley, Phys. Rev. C **9**, 2010 (1974).
- [42] G. Audi, O. Bersillon, J. Blachot, and A. H. Wapstra, Nucl. Phys. **A729**, 3 (2003).
- [43] P. Möller, J. R. Nix, W. D. Myers, and W. J. Swiatecki, At. Data Nucl. Data Tables **59**, 185 (1995).
- [44] V. Yu. Denisov, Phys. Lett. **B526**, 315 (2002).
- [45] V. Yu. Denisov and W. Nörenberg, Eur. Phys. J. A **15**, 375 (2002).
- [46] K. Wildermuth and Y. C. Tang, *A Unified Theory of the Nucleus* (Vieweg, Braunschweig, 1977).
- [47] T. K. Dao and O. M. Knyazkov, Sov. J. Part. Nucl. **21**, 623 (1990).
- [48] B. Nerlo-Pomorska and K. Pomorski, Z. Phys. A **348**, 169 (1994).
- [49] I. Tanihata, D. Hirata, T. Kobayashi, S. Shirnoura, K. Sugimoto, and H. Toki, Phys. Lett. **B289**, 261 (1992).
- [50] R.-D. Herzberg, J. Phys. G **30**, R123 (2004).
- [51] P. Möller, A. J. Sierk, and A. Iwamoto, Phys. Rev. Lett. **92**, 072501 (2004).
- [52] V. Y. Denisov and S. Hofmann, Phys. Rev. C **61**, 034606 (2000).
- [53] A. V. Ignatyuk, M. G. Itkis, V. N. Okolovich, G. N. Smirenkin, and A. S. Tishin, Sov. J. Nucl. Phys. **21**, 612 (1975).